Prediction of Solid-Fluid Equilibria in Supercritical Carbon Dioxide Using Linear Solvation Energy Relationships

David Bush and Charles A. Eckert†

School of Chemical Engineering and Specialty Separations Center
Georgia Institute of Technology, Atlanta, GA 30332-0100, USA

Keywords: supercritical fluid, solid-fluid equilibria, activity coefficient, enthalpy of fusion, LSER

Abstract

Solid-fluid equilibria are important for supercritical fluid processing design. Few data are available, and predictions require a model for the solute-solvent interactions. An activity coefficient model for solids in supercritical CO_2, based on linear solvation energy relationships, is developed. The model fits solubility data at liquid-like densities to a median error of 29 percent. Extrapolations to gas-like densities are shown.

1. Introduction

Designing and costing equipment for supercritical carbon dioxide processing requires phase equilibria data that are usually not available. For extraction or separation of solids using CO_2, the solubility is required for process conditions and scale-up. It is difficult to predict these data from structure alone because two factors are involved, the solute-solute interactions in the solid and solute-solvent interactions in the supercritical fluids. The interactions in the solid are greatest and largely determined from entropic considerations on how well the molecules pack. For example, the solubilities of phenanthrene and anthracene differ by an order of magnitude. In order to avoid the solute-solute interactions in the solid, the sublimation pressure of the solid is used in many models, giving predictions within an order of magnitude. Unfortunately, there are few sublimation pressure data and no easy and accurate techniques exist for measuring very low pressures (less than 1 mPa). An

†Corresponding author

alternative is to use available enthalpy of fusion data, used in the prediction of solubility in liquids.

The prediction of solid-liquid equilibria is well established [1, 2]. The solubility model requires the enthalpy and temperature of fusion for the solid and the activity coefficient of the solute in solution. The fusion temperature is available for virtually all solids except those that decompose before melting. Enthalpy of fusion data are abundant in the literature [3, 4], or they can be quickly measured in a differential scanning calorimeter [5]. Since the solubility of solids in liquids is usually insensitive to the quality of the solution model, an ideal solution model often performs adequately. For solids of low solubility (usually those with high melting points) solute-solvent interactions are significant, and an appropriate activity coefficient model must be chosen. The ideal solution predicts solubilities 10 to 1000 times greater than those found in CO_2. For liquids, there are a number of good activity coefficient models, such as UNIFAC [6], ASOG [7], and SPACE [8]. These models have been incorporated as mixing rules in equations of state, but the formulations still require sublimation pressure data.

In this paper, supercritical carbon dioxide is treated as an expanded liquid. The derivation of solid solubility using the same formulation as in liquids is shown, previous activity coefficient models are evaluated, and a new predictive method is derived.

2. Solubility model

In this formulation, component 2 will be the solid and component 1 will be the solvent, CO_2. The condition for equilibrium is that the fugacity of each component must be equal in both phases. For the solid, this gives

$$f_2^S = f_2^L \tag{1}$$

where f_2^S is the fugacity of the pure solid and f_2^L is the fugacity of the hypothetical subcooled liquid in solution. The standard state is defined as the system temperature and some pressure, P^0. The fugacity of the pure solid can then be expressed in terms of the fugacity at the standard state, $f_2^S(P^0)$, by equation (2).

$$f_2^{\ S} = f_2^{0S}\left(P^0\right)\exp\left[\int_{P^0}^{P}\frac{v_2^S \mathrm{d}P}{RT}\right] \qquad \textbf{(2)}$$

The exponential term is the Poynting correction, and it can be simplified by assuming that the solid is incompressible. The fugacity of the subcooled liquid is also expressed in terms of the fugacity at the standard state.

$$f_2^{\ L} = y_2\gamma_2 f_2^{0L}\left(P^0\right)\exp\left[\int_{P^0}^{P}\frac{v_2^L \mathrm{d}P}{RT}\right] \qquad \textbf{(3)}$$

If v_2^L is assumed constant with pressure and equal to v_2^S, then combining equations (1), (2), and (3) gives

$$y_2 = \frac{1}{\gamma_2}\frac{f_2^{0S}\left(P^0\right)}{f_2^{0L}\left(P^0\right)} \qquad \textbf{(4)}$$

The ratio of the standard state fugacities is only dependent on the properties of the solute. Prausnitz et al. [1] have derived this ratio in terms of measurable properties with

$$\frac{f_2^{0S}\left(P^0\right)}{f_2^{0L}\left(P^0\right)} = \frac{1}{RT^2}\int_{T_2^{tp}}^{T}\left(\Delta H_2^{tp} + \int_{T_{tp}}^{T}\Delta C_{p,2}^{tp}dT\right)dT - \frac{1}{RT}\int_{P_2^{tp}}^{P^0}\Delta v_2^{tp}dP \qquad \textbf{(5)}$$

where the superscript *tp* refers to the triple point, but can be replaced by the melting point with little loss of error. For many solids, ΔH^{fus} is between 4000 and 10,000 cal/mol, ΔC_P^{fus} is between 0 and 10 cal/mol, and Δv^{fus} is between 0 and 15 cm^3/mol. The terms that include

ΔC_P and Δv are much smaller than ΔH^{fus} and, at moderate pressures, tend to cancel each other out, leaving a much simpler expression shown in equation (6).

$$\frac{f_2^{0S}\left(P^0\right)}{f_2^{0L}\left(P^0\right)} = \exp\left[\frac{\Delta H_2^{fus}}{R}\left[\frac{1}{T_2^{fus}} - \frac{1}{T}\right]\right] \qquad \textbf{(6)}$$

Combining equations (4) and (6) give

$$y_2 = \frac{1}{\gamma_2^{\infty}}\exp\left[\frac{\Delta H_2^{fus}}{R}\left[\frac{1}{T_2^{fus}} - \frac{1}{T}\right]\right] \qquad \textbf{(7)}$$

Since the solubilities in CO_2 are low, we assume that γ_2 is independent of concentration and equal to γ_2^{∞} .

Activity coefficients calculated from solubility data using equation (7) are shown in **Figure 1** for ketoprofen. The activity coefficients are large, greater than 10^4, and vary with both temperature and pressure. It should be noted that the error in γ depends on the errors in the solubility and in the heat of fusion, with errors increasing with T-T_2^{fus}. For comparison, the activity coefficient of ketoprofen in acetone at saturation is 1.03 [9].

3. Regular solution theory model

To predict solubilities using equation (7) requires an activity coefficient model that applies to CO_2 and the diverse solids. Hildebrand regular solution theory combined with Flory-Huggins theory is one method that has been applied to supercritical fluids [10, 11].

$$\ln\gamma_2^{\infty} = \frac{v_2}{RT}\left[\delta_1 - \delta_2\right]^2 + 1 - \frac{v_2}{v_1} + \ln\frac{v_2}{v_1} \qquad \textbf{(8)}$$

where δ_1 and δ_2 are the solubility parameters for the solvent and the solute. Because δ_2 is the solubility parameter of a hypothetical liquid, it must be extrapolated from liquid data [12] or estimated. In this work, the group contribution technique of Fedors was used [13].

For the supercritical solvent, an equation of state is used for the evaluation of δ_1 [14, 15]. The expression of δ for an equation of state explicit in pressure is

$$\delta_1 = \sqrt{\rho \int_0^{\rho} \left\{ \frac{P}{\rho^2} - \frac{T}{\rho^2} \left[\frac{\partial P}{\partial T} \right]_{\rho} \right\} \mathrm{d}\rho} \qquad \textbf{(9)}$$

An analytical expression was derived using the 32-parameter Jacobsen and Stewart equation regressed by Ely *et al* [16].

To test the capability of this RST-FH model, equations (8) and (7) were used to predict the solubility of several solids in CO_2. Shown in **Figure 2** are the predictions for 2,4-dichlorophenoxyacetic acid. The model, shown as solid lines, has the wrong temperature and density dependence, but it does give a qualitative picture because the solubility parameter of CO_2 is linearly related to the density of CO_2.

To ameliorate the deficiencies in regular solution theory, Kramer and Thodos added a binary interaction parameter, β_{12}, which accounts for the polar and hydrogen-bonding contributions from the solute and solvent. To fit solubility data for octadecanol and octadecanoic acid, they found that β_{12} was not constant and needed **9** parameters for each solid to be within the experimental error [17]. Iwai et al. [11] found better results by constraining v_2 to the following relationship:

$$\ln v_2 = a \ln \rho_1 + b \qquad \textbf{(10)}$$

This approach requires only 2 parameters per binary pair and forces. Neither result netted a predictive method.

Since the solubility parameter of CO_2 is linearly related to its density, a better test of regular solution theory would be to compare predictions at a fixed temperature and pressure. The activity coefficient for 47 solids at 35°C and 150 bar, calculated from

solubility data and equation (7), has no discernable correlation with solubility parameter of the solid as shown in **Figure 3**. An alternative to regular solution theory will be proposed.

4. Linear solvation energy relationship

The regular solution theory approach tries to the combine the pressure dependence, temperature dependence, and compound variability in one simple form. The problem can be examined better by separating the dependencies of pressure, temperature, and compound. We present a method for predicting the activity coefficient at a reference pressure and temperature and show how to extrapolate to other conditions. We chose 35°C as the reference temperature since more data are available at this temperature than at any other. The reference pressure was chosen to give an arbitrary liquid-liquid density of 21 mol/L. At 35°C, the reference pressure is 28.9 MPa.

For the compound dependence on $\gamma(P^0)$, activity coefficients were back-calculated from solubility data. The LSER method, developed by Kamlet, Taft, and collaborators [18] and used by Sherman *et al.* for the prediction of activity coefficients in water [19] was tested for regression of the data. The LSER assumes that some property is linearly related to an orthogonal set of parameters as shown in equation (11)

$$XYZ = \xi_0 + \xi_1\pi^* + \xi_2\alpha + \xi_3\beta + \xi_4 \log L^{16} \qquad \textbf{(11)}$$

where *XYZ* is some configurational property, ξ_i are coefficients or adjustable parameters, π^* is a scale of the polarity/polarizability, α is the scale for hydrogen bonding acidity, β is the scale for hydrogen bonding basicity, and L^{16} is the hexadecane-air partition coefficient which represents hydrophobicity. Because L^{16} values are not available for most of the solids in this study, McGowen's intrinsic volume [20], which is correlated with L^{16}, was used instead. The following function,

$$\ln \gamma_2^{\infty} = (2.64 \pm 0.36)\pi_2^* + (1.85 \pm 0.70)\alpha_2^H + (1.13 \pm 0.28)V_x \quad \textbf{(12)}$$

fit ln γ_2 with an average error of 9 percent and γ_2 with a median error of 27 percent. Given that solubility, at best, is good to within 20 percent and that heat of fusion data are accurate to 10 percent, this is considered a good fit. The coefficient for β was insignificant, even though carbon dioxide can act as a Lewis acid [21]. Ikushima et al. have showed that α for carbon dioxide, which should be related to ξ_3, decreases with pressure and is negative at liquid-like densities [22]. A plot of γ_2 versus V_x is shown in **Figure 4** for compounds with no protic hydorgen.

The relationship between activity coefficient and pressure is defined in terms of partial molar quantities,

$$\left[\frac{\partial \ln \gamma_i}{\partial P}\right]_{T,y} = \frac{\bar{v}_i - v_i}{RT} \quad \textbf{(13)}$$

where v is the molar volume and the bar above the variable denotes a partial molar quantity. Near the critical density, $\bar{v}_2$ is large and negative, indicating that the solvent is collapsing around the solute molecules. This behavior is similar for compounds in supercritical fluids. Including the pressure dependence of the activity coefficient from equation (13) in equation (4) gives the following function for solubility:

$$y_2 = \frac{f_2^{0S}(P^0)\exp\left[\dfrac{v_2^S\left[P - P^0\right]}{RT}\right]}{\gamma_2^{\infty}(P^0) f_2^{0L}(P^0)\exp\left[\displaystyle\int_{P^0}^{P} \frac{\bar{v}_2 \, \mathrm{d}P}{RT}\right]} \quad \textbf{(14)}$$

where $\gamma_2(P^0)$ is the activity coefficient at P^0. Note that the Poynting corrections no longer cancel. Applying equation (14) requires γ_2 at one pressure and either a model or data for $\bar{v}_2$.

Partial molar volume data can be measured from density measurements [23, 24] or chromatography [25, 26] or estimated from an equation of state. The chromatographic approach is the quicker and simpler measurement. The Peng-Robinson equation of state can be used to regress partial molar volume data with one adjustable parameter [24]. It fails near the critical point, but because our model starts at a high-pressure reference point, it does an adequate job of regressing solubilities. Shown in Figure 5 are two models fitted to phenanthrene solubility data. The solid line is equation (14) with the Peng-Robinson equation of state used for the partial molar volume. The dotted line is the compressed gas model with the Peng-Robinson used for the fugacity coefficient. When the Peng-Robinson is used strictly for the partial molar volume, the model can describe the measured data within the measurement error and with no systematic bias.

As Eckert et al. [24] pointed out, the partial molar volume scales with the compressibility of the supercritical fluid. A very simple model for $\bar{v}_2$ is

$$\bar{v}_2 = v_2^S - A\kappa RT\rho \qquad \textbf{(15)}$$

where A is an adjustable parameter, κ is the compressibility, and v_2^s is the molar volume of the solid. This model implies log y varies linearly with ρ with A being the slope [27, 28].

Applying equation (15) to equation (14) simplifies to

$$y_2 = \frac{f_2^{0S}\left(P^0\right) / f_2^{0L}\left(P^0\right)}{\gamma_2^{\infty}\left(P^0\right)\exp\left[-A\left[\rho - \rho\left(P^0\right)\right]\right]} \qquad \textbf{(16)}$$

where $\rho(P^0)$ is the density at P^0. Note that equation (16) has the pressure dependence built into the model. To use it in a predictive matter requires the temperature and compound dependence on A and $\gamma(P^0)$. These parameters were determined for 63 compounds and are listed in **Table 1**. The reference density, $\rho(P^0)$, was set to 21 mol/L.

The parameter A in equation (16) has a mean of 280 cm^3/mol with half the values between 225 and 325 cm^3/mol. Because A is a derivative property of solubility data, the uncertainty associated with it is higher than the error in the solubility data; therefore, most of the variation in A is from random error. A small portion of the variation can be explained by examining the dependence on the system temperature, size of the molecule, and polarity of the solid to give

$$A = 817 + 0.553\,\mathrm{V_x} + 78.9\,\pi_2^* - 746\,\frac{\mathrm{T_c}}{\mathrm{T}} \qquad \textbf{(17)}$$

where V_x is McGowen's intrinsic volume in cm^3/mol, π_2^* is the solute polarity/polarizability from the Abraham scale, and T_c is the critical temperature. Equation (17) has an average error of 42 percent.

The temperature dependence of the activity coefficient is defined in equation (18)

$$\left[\frac{\partial \ln \gamma_i}{\partial 1/T}\right]_{P,y} = \frac{h_i - \bar{h}_i}{R} = \frac{\bar{h}_i^E}{R} \qquad \textbf{(18)}$$

where h is the molar enthalpy, the bar denotes a partial molar quantity, and the superscript E is an excess property. There are numerous data for partial molar excess enthalpies in liquid solvents using flow calorimeters [29, 30] but few involving CO_2 as the solvent [31]. In lieu of data, the partial molar enthalpies were calculated from the activity coefficients listed in **Table 1**. The average of $\bar{h}_2^E$ for the data set is 31 kJ/mol with half the data

between 20 and 45 kJ/mol. For comparison, $\bar{h}_2^E$ for 1-alkanols in cyclohexane are approximately 24 kJ/mol. Sherman *et al.* found that partial molar enthalpies could be correlated using linear solvation energy relationships [32]. For a particular solvent,

$$\bar{h}_2^{E^\infty} = \Delta h_2^{vap} + \xi_0 + \xi_1 \log L_2^{16} + \xi_2 \pi_2^* + \xi_3 \alpha_2 + \xi_4 \beta_2 \qquad \textbf{(19)}$$

where Δh_2^{vap} is the heat of vaporization. Sherman's correlation is solvent specific with parameters determined for 18 different liquid solvents. Attempts to correlate $\bar{h}_2^E$ in CO_2 using equation (19) yielded no statistically significant coefficients. This is expected since $\bar{h}_2^E$ is calculated from highly variable data within a narrow temperature range of 35 to 65°C.

The solubility of phenanthrene will be used as a sample calculation. Using equation (17) gives A = 260 cm^3/mol, equation (12) give γ_2 = 156 at 35°C, and assuming $\bar{h}_2^E$ = 31 kJ/mol. The entire solubility behavior can be determined as shown in **Figure** 6. The comparisons for polar compounds will not be as good.

5. Conclusion

The solubility of solids in supercritical fluids can be described adequately using the expanded liquid model. The model can be used to predict on the basis of available pure component properties or affords an excellent means of extrapolating limited solubility data. This model provides the framework for expanding to cosolvent systems. The activity coefficient model just requires a dependence on cosolvent concentration.

6. Nomenclature

List of Symbols

a adjustable parameter
A adjustable parameter
b adjustable parameter

f	fugacity
ΔH	change in enthalpy
k	adjustable parameter
L^{16}	hexadecane-air partition coefficient
P	pressure
R	universal gas constant
T	temperature
V_x	McGowen's intrinsic volume
v	molar volume
$\bar{v}$	partial molar volume
y	mole fraction
α	acidity parameter
β	basicity parameter
γ	activity coefficient
δ	Hildebrand solubility parameter
κ	isothermal compressibility
π^*	polarity/polarizability parameter
ρ	density
τ	Hansen's solubility parameter due to polar and hydrogen bonding
ξ	adjustable parameter in LSER

List of subscripts

1	carbon dioxide
2	solute
C	critical
R	reduced

List of superscripts

0	reference state
D	due to dispersion forces only
fus	fusion
i.g.	ideal gas
L	liquid phase
tp	triple point
S	solid phase
vap	vaporization

7. Acknowledgements

The authors gratefully acknowledge financial support from the E.I. DuPont Nemours Co. and the United States Department of Energy.

8. References

[1] J.M. Prausnitz, R.N. Lichtenthaler and E.G. de Azevedo *Molecular Thermodynamics of Fluid-Phase Equilibria*, 2nd ed.; Prentice Hall: Englewood Cliffs, N. J., 1986.

[2] S.M. Walas *Phase Equilibrium in Chemical Engineering*; Butterworth: Boston, 1985.

[3] E.S. Domalski, W.H. Evans and E.D. Hearing, J. Phys. Chem. Ref. Data, 13, Supp. No. 1 (1984) 1-286.

[4] E.S. Domalski and E.D. Hearing, J. Phys. Chem. Ref. Data, 19 (1990) 881-1047.

[5] J.R. Donnelly, L.A. Drewes, R.L. Johnson, W.D. Munslow, K.K. Knapp and G.W. Sovocool, Thermochim. Acta, 167 (1990) 155-187.

[6] J. Gmehling, J. Li and M. Schiller, Ind. Eng. Chem. Res., 32 (1993) 178-193.

[7] K. Tochigi, D. Tieges, J. Gmehling and K. Kojima, J. Chem. Eng. Japan, 23 (1990) 453-463.

[8] M.J. Hait, C.L. Liotta, C.A. Eckert, D.L. Bergmann, A.M. Karachewski, A.J. Dallas, D.I. Eikens, J.J. Li, P.W. Carr, R.B. Poe, S.C. Rutan, Ind. Eng. Chem. Res., 32 (1993) 2905-2914.

[9] F. Espitalier, B. Biscans and C. Laguérie, J. Chem. Eng. Data, 40 (1995) 1222-1224.

[10] A. Kramer and G. Thodos, Ind. Eng. Chem. Res., 27 (1988) 1506-1510.

[11] Y. Iwai, Y. Koga, T. Fukuda and Y. Arai, J. Chem. Eng. Jpn., 25 (1992) 757-760.

[12] D.H. Ziger and C.A. Eckert, Ind. Eng. Chem. Process Des. Dev., 22 (1983) 582-588.

[13] R.F. Fedors, Polym. Eng. Sci., 14 (1974) 147-154.

[14] S.R. Allada, Ind. Eng. Chem. Process Des. Dev., 23 (1984) 344-348.

[15] T.-H. Pang and E. McLaughlin, Ind. Eng. Chem. Process Des. Dev., 24 (1985) 1027-1032.

[16] J.F. Ely, W.M. Haynes and B.C. Bain, J. Chem. Therm., 21 (1989) 879-894.

[17] A. Kramer and G. Thodos, J. Chem. Eng. Data, 34 (1989) 184-187.

[18] M.J. Kamlet, J.-L.M. Abboud, M.H. Abraham and R.W. Taft, J. Org. Chem., 48 (1983) 2877-2887.

[19] S.R. Sherman, D.B. Trampe, D.M. Bush, M. Schiller, C.A. Eckert, A.J. Dallas, J. Li and P.W. Carr, Ind. Eng. Chem. Res., 35 (1996) 1044-1058.

[20] M.H. Abraham and J.C. McGowan, Chromatographia, 23 (1987) 243-246.

[21] S. Kazarian, M.F. Vincent, F.V. Bright, C.L. Liotta and C.A. Eckert, J. Am. Chem. Soc., 118 (1996) 1729-1736.

[22] Y. Ikushima, N. Saito, M. Arai and K. Arai, Bull. Chem. Soc. Jpn., 64 (1991) 2224-2229.

[23] C.A. Eckert, D.H. Ziger, K.P. Johnston and T.K. Ellison, Fluid Phase Equilib., 14 (1983) 167-175.

[24] C.A. Eckert, D.H. Ziger, K.P. Johnston and S. Kim, J. Phys. Chem., 90 (1986) 2738-2746.

[25] J.J. Shim and K.P. Johnston, J. Phys. Chem, 95 (1991) 353-360.

[26] Z.S. Gönenç, U. Akman and A.K. Sunol, J. Chem. Eng. Data, 40 (1995) 799-804.

[27] S.K. Kumar and K.P. Johnston, J. Supercrit. Fluids, 1 (1988) 15-22.

[28] H. Liu and E.A. Macedo, Ind. Eng. Chem. Res., 34 (1995) 2029-2037.

[29] D.M. Trampe and C.A. Eckert, J. Chem. Eng. Data, 36 (1991) 112-118.

[30] T. Pfeffer, B. Löwen and S. Schulz, Fluid Phase Equil., 106 (1995) 139-167.

[31] A. Stassi and A. Schiraldi, Thermochimica Acta, 246 (1994) 417-425.
[32] S.R. Sherman, D. Suleiman, M.J. Hait, M. Schiller, C.L. Liotta, C. Eckert, A., J. Li, P.W. Carr, R.B. Poe and S.C. Rutan, J. Phys. Chem., 99 (1995) 11239-11247.
[33] S.J. Macnaughton, I. Kikic, N.R. Foster, P. Alessi, A. Cortesi and I. Colombo, J. Chem. Eng. Data, 41 (1996) 1083-1086.
[34] S.J. Macnaughton and N.R. Foster, Ind. Eng. Chem. Res., 33 (1994) 2757-2763.
[35] J.M. Dobbs, J.M. Wong and K.P. Johnston, J. Chem. Eng. Data, 31 (1986) 303-308.
[36] R.T. Kurnik, S.J. Holla and R.C. Reid, J. Chem. Eng. Data, 26 (1981) 47-51.

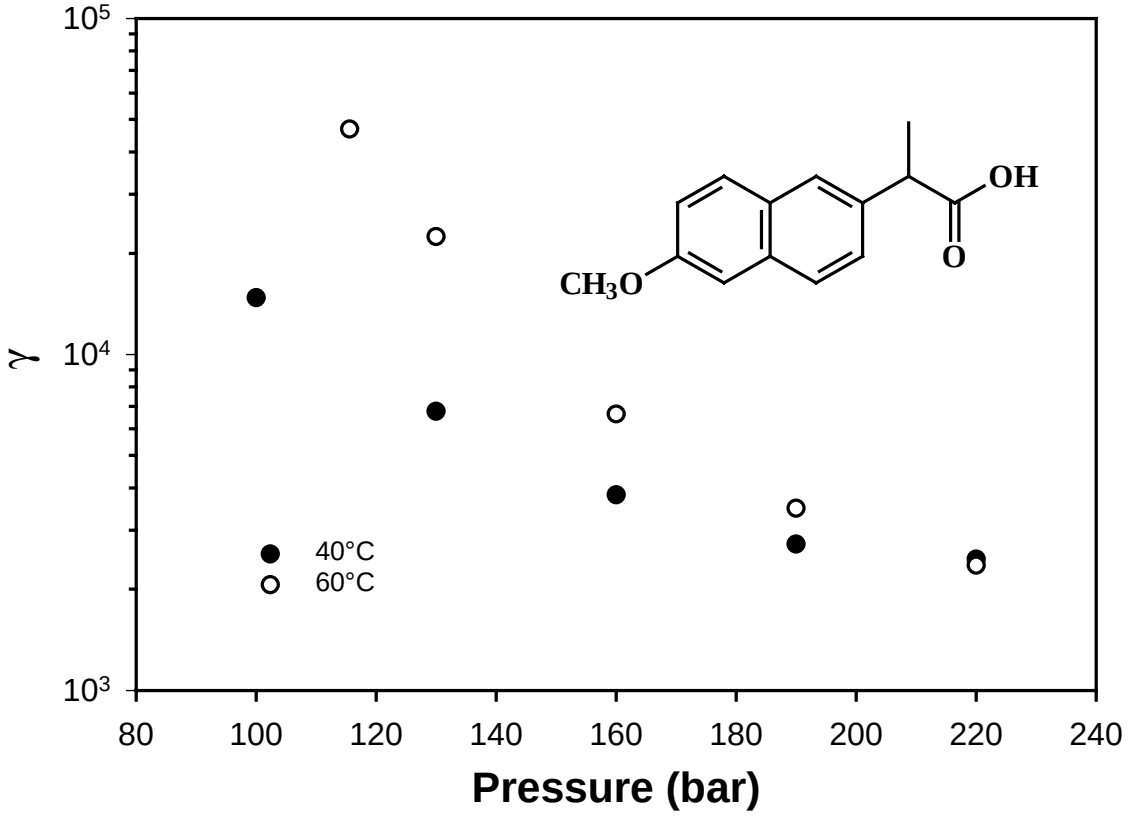

Figure 1. Activity coefficient of ketoprofen in CO_2. Data from Macnaughton et al. [33].

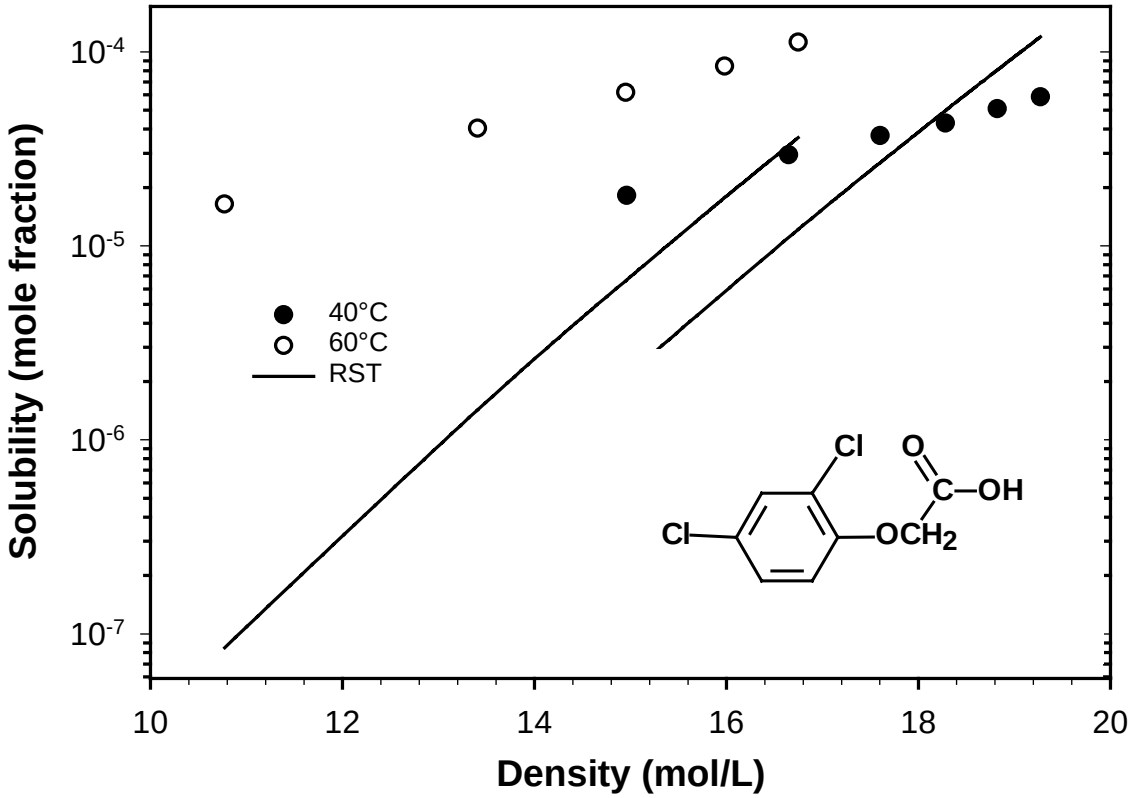

Figure 2. Comparison of regular solution theory to predict the solubility of 2,4-D in CO_2. Data from McNaughton and Foster, 1994 [34].

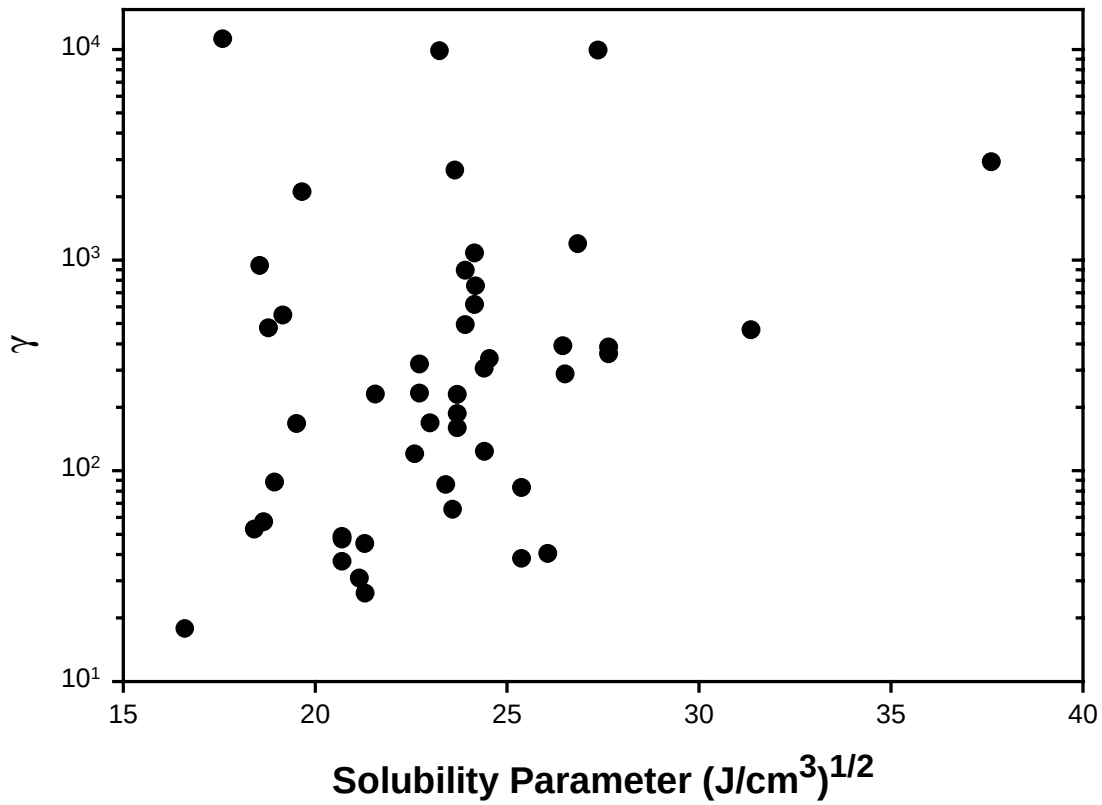

Figure 3. Variation in γ with solute solubility parameter at 35°C and 150 bar.

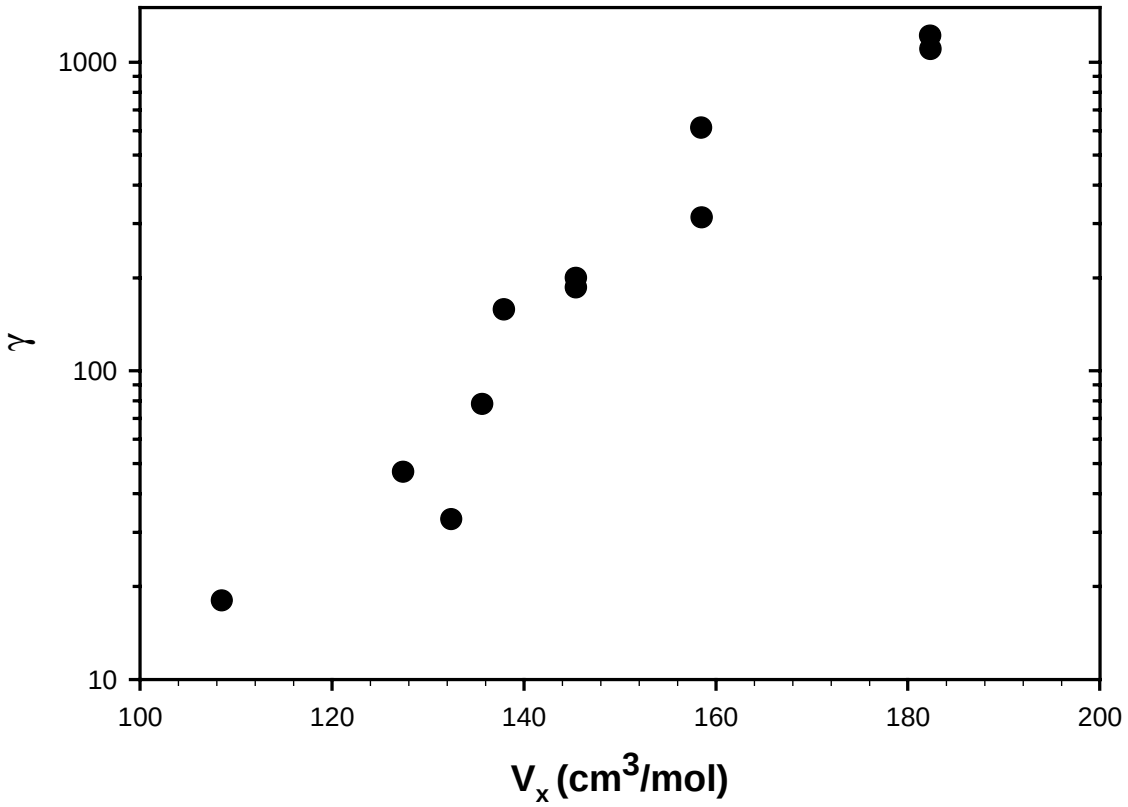

Figure 4. Activity coefficients versus intrinsic volume.

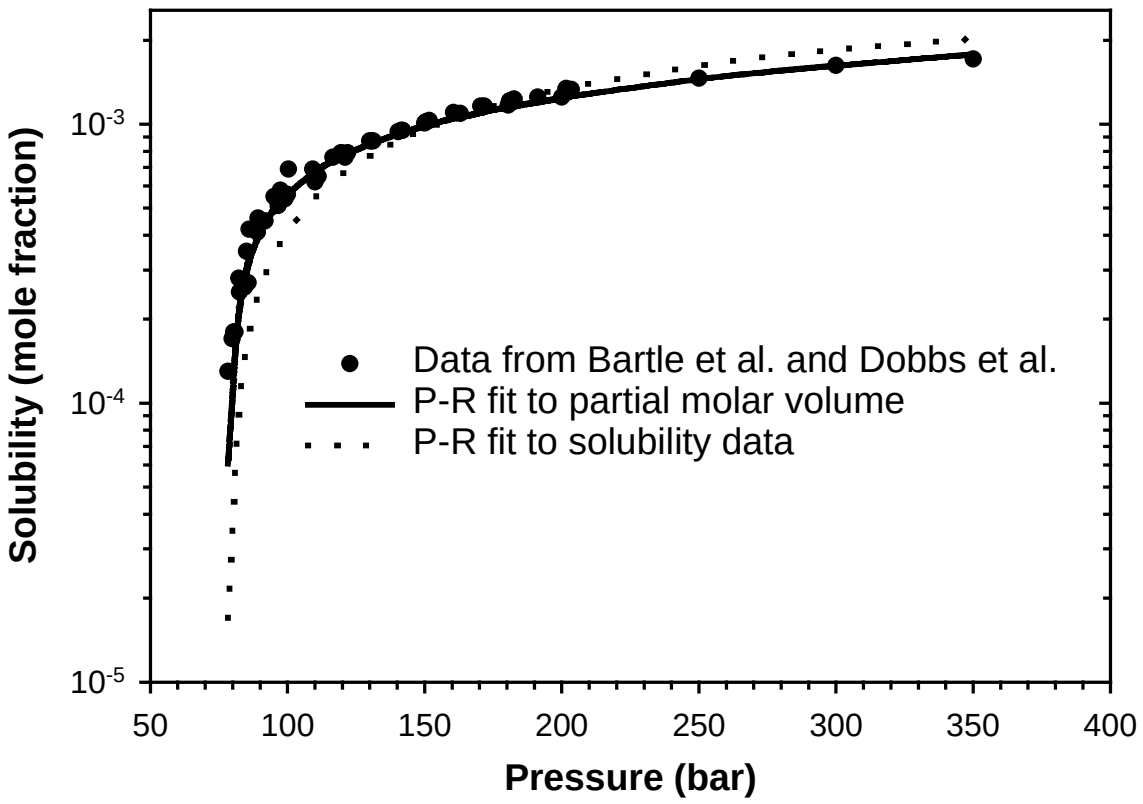

Figure 5. Comparison of partial molar volume data to fugacity coefficient prediction.

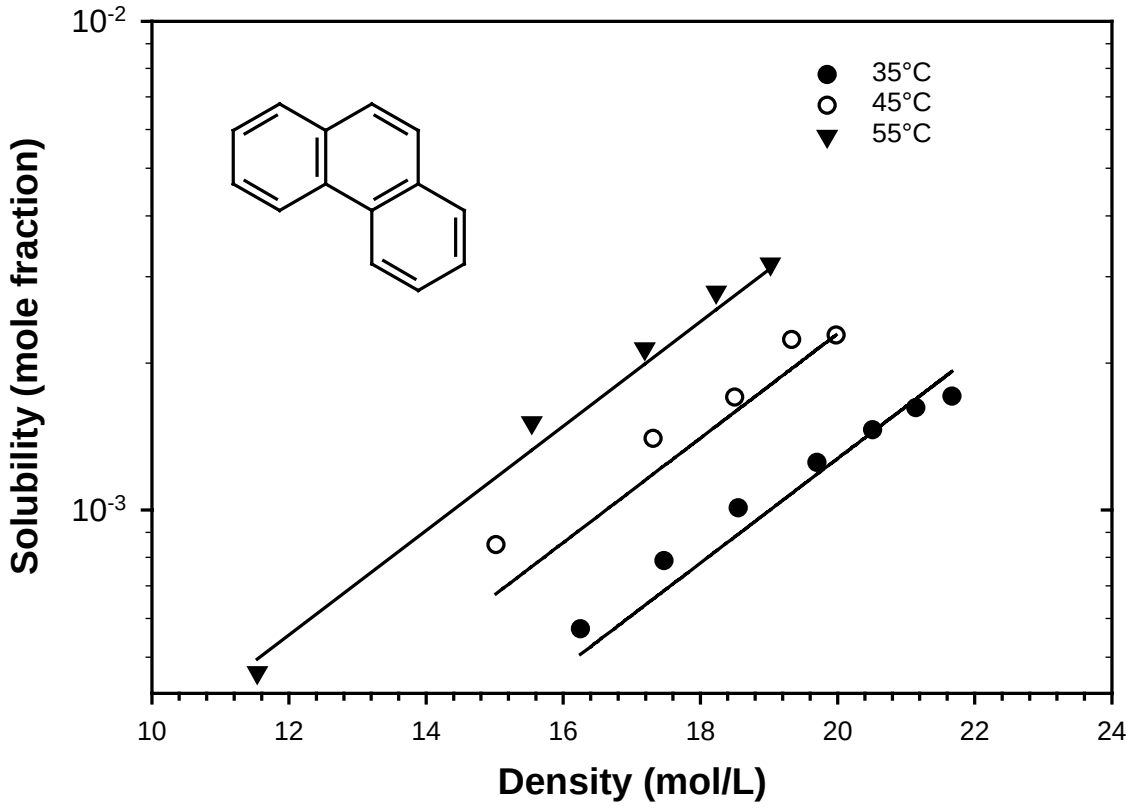

Figure 6. Comparison of expanded liquid model with phenanthrene solubility data. Data from Dobbs et al. and Kurnik et al. [35, 36].

Table 1. Coefficients for expanded liquid model.

Solid	**T (K)**	**$\gamma(P^0)$**	***A*** (cm^3/mol)
acridine	308	291	286
	318	150	311
	323	285	322
	328	107	329
	343	80	330
aminobenzoic acid, 2-	308	847	152
anthracene	313	186	164
	323	157	202
	333	119	248
benzoic acid	308	65	261
	318	41	316
	328	27	328
	338	14	369
	343	14	345
biphenyl	309	33	79
caffeine	313	80	270
	333	61	270
	353	36	308
6-caprolactam	307	4	460
	314	3	559
	324	6	315
carbazole	313	420	183
beta-carotene	313	2505	512
	323	1992	526
cholesterol	308	761	416
	313	245	344
	323	459	179
	328	173	324
	333	212	296
chrysene	308	1220	347
2,4-D	313	411	265
	323	335	264
	333	200	316
DDT	313	139	309
	323	88	371
	333	42	449
diamantane	333	24.5	264
dibenzofuran	308	47	304
	323	25	278
	343	11	355
dibenzothiophene	308	158	270
	323	151	300
	328	65	322
	338	44	348
	343	62	315
dimethylnaphthalene, 2,3-	308	24	222
	318	23	200
	328	16	285
dimethylnaphthalene, 2,6-	308	36	117
	318	22	240
	328	15	259

Solid	**T (K)**	**$\gamma(P^0)$**	***A*** (cm^3/mol)
dimethylnaphthalene, 2,7-	308	35	135
	328	15	248
eicosanoic acid	308	387	387
	318	456	337
	328	467	227
1-eicosanol	308	373	139
	318	169	231
	328	51	351
ferrocene	313	37	195
	323	31	202
	333	26	219
	343	20	243
fluoranthene	308	314	288
	318	179	354
	328	91	402
fluorene	308	78	197
	313	72	164
	318	49	269
	323	36	304
	328	31	300
	343	28	294
glucose	308	1156	191
	328	8042	-5
	348	13656	-13
hexachloroethane	308	17	56
	318	11	118
	328	5.6	201
hexadecanol	308	103	209
	318	55	286
	328	51	360
	333	57	377
hexamethylbenzene	308	47	49
	323	20	276
	343	16	254
hydroquinone	308	7055	150
	318	5673	134
hydroxybenzoic acid, o-	308	240	256
	313	187	272
	318	127	317
	328	90	300
ketoprofen	313	1370	375
	332	576	393
lindane	313	69	250
	333	24	378
methoxybenzoic acid, 2-	308	267	252
	318	197	278
	328	142	292
methoxybenzoic acid, 4-	308	529	213
	318	426	243
	328	276	289
methoxychlor	313	213	312

Solid	**T** (K)	$\gamma(P^0)$	***A***(cm^3/mol)
methoxychlor	333	45	494
methylbenzoic acid, 2-	313	89	241
	323	49	272
	333	24	327
methylbenzoic acid, 3-	313	94	243
	323	55	285
	333	26	347
methylbenzoic acid, 4-	313	130	212
	323	89	251
	333	55	289
myristic acid	308	49	301
	313	19	467
naphthalene	308	18	146
	318	10	236
	323	11	206
	328	7.1	227
1-naphthol	308	162	273
	318	110	256
	328	82	256
2-naphthol	308	283	207
	318	220	203
	328	140	240
	343	235	263
naphthaquinone, 1,4-	318	26	224
	328	19	286
	343	11	326
naproxen	313	879	308
	323	672	311
	333	678	278
octacosane	308	1159	200
	313	900	250
	318	400	329
	323	335	241
octadecanol	308	167	219
	318	87	233
	328	43	342
	338	47	381
palmitic acid	308	252	284
	313	75	557
	318	37	409
	328	31	434
	338	26	481
perylene	313	10610	1085
	373	597	501
phenanthrene	308	200	209
	313	221	173
	318	115	250
	323	78	304
	328	58	324
	338	63	270
	343	100	231
phenazine	323	59	364
phthalic anhydride	308	39	228
progesterone	308	87	501
	313	69	548

Solid	**T** (K)	$\gamma(P^0)$	***A***(cm^3/mol)
progesterone	318	74	443
	328	49	514
pyrene	308	614	247
	318	426	282
	323	352	298
	328	290	305
	343	185	358
stearic acid	308	505	312
	318	199	17
	328	43	426
testosterone	308	703	414
	313	466	600
	318	322	612
	328	552	357
	373	163	352
theobromine	313	222	368
	333	272	159
	353	333	135
	368	446	212
theophylline	313	497	100
	333	606	57
	353	467	149
thianthrene	323	140	368
	343	118	334
triphenylene	308	1104	309
	318	706	357
	328	501	377
triphenylmethane	323	160	136
	343	132	218
xylenol, 2,5-	308	62	137
xylenol, 3,4-	308	56	163